PHYSICAL REVIEW B

CONDENSED MATTER

THIRD SERIES, VOLUME 45, NUMBER 18 1 MAY 1992-II

Infrared studies of the phase transition in the organic charge-transfer salt *N*-propylquinolinium ditetracyanoquinodimethane

J. L. Musfeldt
Department of Chemistry, University of Florida, Gainesville, Florida 32611

K. Kamarás
Central Research Institute for Physics, H 1525 Budapest, Hungary

D. B. Tanner
Department of Physics, University of Florida, Gainesville, Florida 32611
(Received 9 October 1991; revised manuscript received 23 December 1991)

Polarized infrared and optical reflectance spectroscopies were used to study the structural phase transition in the organic charge-transfer salt *N*-propylquinolinium ditetracyanoquinodimethane. Above the 220-K phase-transition temperature, the spectra are characteristic of other 1:2 semiconducting charge-transfer salts. Three significant changes occur below T_c. First, the midinfrared charge-transfer band can be resolved into two distinct excitations. Second, there is enhanced oscillator strength, indicative of a larger intratetramer transfer integral in the low-temperature phase. Finally, the vibrational lines split into doublets, providing evidence for an uneven charge distribution within the tetramer. The weakly metallic transport properties above T_c are attributed to the uniform charge distribution within the tetramer and the high degree of overlap between the intratetramer and intertetramer charge-transfer bands. The transport properties in the low-temperature phase are dominated by charge localization, which may act to reduce the overlap between these low-energy charge-transfer features.

I. INTRODUCTION

N-propylquinolinium ditetracyanoquinodimethane [NPrQn(TCNQ)$_2$] is a 1:2 organic charge-transfer salt containing segregated chains of TCNQ tetramers and NPrQn counterions. The stoichiometric ratio of the donor to acceptor entities is such that NPrQn(TCNQ)$_2$ is referred to as a "quarter-filled" charge-transfer salt. It undergoes a second-order structural metal-semiconductor transition at a critical temperature (T_c) of 220 K.[1,2]

The 1:2 charge-transfer salts are generally semiconductors as a result of a structural distortion, which distorts the uniform intermolecular spacing and introduces gaps in the metallic band structure.[3–6] However, the transport properties of NPrQn(TCNQ)$_2$ have been described as weakly metallic, with a value[1] for the dc conductivity of approximately 1 $\Omega^{-1}\,\mathrm{cm}^{-1}$. An explanation for this unusual metallic conductivity above T_c was proposed by Jánossy *et al.*,[2] who suggested that the Coulomb interaction of the donor cations and the TCNQ chains could perturb the band structure in the TCNQ stack, resulting in enhanced conductivity. Below T_c, the dc conductivity drops sharply by about 4 orders of magnitude.[1] In this case, conduction in NPrQn(TCNQ)$_2$ has been shown to proceed by excitation over a temperature dependent gap,[2] as in an ordinary semiconductor.

Structural studies[7,8] of this material reveal several important features. The intratetramer distances change significantly between the high-temperature and low-temperature phase. At 300 K, intratetramer distances of 3.24 and 3.28 Å are reported, while at 100 K, these distances decrease to a uniform 3.15 Å. Thus, at low temperature, the TCNQ chains become more uniformly tetramerized. In contrast, the intertetramer distances are temperature independent, remaining constant at 3.43 Å, resulting in relatively well-isolated tetramers within the TCNQ stack. The $P\bar{1}$ space group, the mode of overlap within the tetramer, and the intramolecular bond lengths and angles remain unaffected by the phase transition. Based upon the structural data, it has been concluded that the crystal structure becomes more uniform at low temperature.[8] However, this conclusion is in direct contradiction with low-temperature measurements of other physical properties,[1,2] which indicate a *less* uniform charge distribution within the tetramer below T_c.

The phase transition causes important changes in the

magnetic state of NPrQn(TCNQ)$_2$.[1,2] Paramagnetic susceptibility (χ) measurements show that χ is large and constant in the high-temperature phase, corresponding to 0.8% free spins per formula unit. Between 200 and 80 K, there is a strong decrease in the susceptibility, which is characteristic of a singlet ground state with a low-lying triplet spin excitation. EPR measurements also confirm the formation of triplet states below 100 K. The energy gap between the singlet and triplet states increases with decreasing temperature. At low temperature, χ is small; below 80 K, a Curie tail appears. On the basis of these observations, it has been suggested that magnetic interactions may be the driving force for the structural phase transition.[1,2]

The dielectric constant,[1] measured at 9.1 GHz, is constant at approximately 6 in the high-temperature phase. Between 240 and 180 K, it gradually decreases to a final value of 2 in the low-temperature phase.

In order to provide further information on the nature of the high- and low-temperature phase, we have investigated the optical properties of *N*-propylquinolinium (TCNQ)$_2$. Optical methods are well suited to the study of such highly anisotropic crystals, providing information on both the electronic charge transfer and localized excitations at high energies as well as the vibrational features at lower energies.[3–6] Ten infrared-active vibrational modes in the TCNQ chain direction are of particular interest. Infrared activity of these modes[9–11] is attributed to the coupling of the totally symmetric (A_g) TCNQ phonon modes with the low-lying electronic charge-transfer excitation, and is very sensitive to changes in the electronic structure of the crystal. Emphasis has been placed on the correlation of the spectral properties above and below T_c with available structural and transport data with the goal of obtaining a greater understanding of the characteristics of the phase transition. In addition, we compare our data on NPrQn(TCNQ)$_2$ to previous results on the closely related compounds Qn(TCNQ)$_2$ and (NMP)x(Phen)$_{1-x}$(TCNQ) by McCall *et al.*[12]

II. EXPERIMENT

Near normal polarized reflectance measurements were made on single-crystal samples of NPrQn(TCNQ)$_2$. Far-infrared (FIR) and midinfrared (MIR) measurements were carried out on an IBM-Bruker 113v Fourier-transform infrared spectrometer from 30 to 5000 cm^{-1}. In the FIR, a liquid-helium-cooled Si bolometer (Infrared Laboratories LN-6/C) was used as the detector. In the MIR, a DTGS detector was used. Wire grid polarizers on polyethylene and AgBr were used in the FIR and MIR, respectively. A Perkin-Elmer grating spectrometer was used to measure the spectra in the infrared to the ultraviolet (1000–30 000 cm^{-1}), using wire grid and dichroic polarizers. The complete apparatus and its operation has been described elsewhere.[13] For low-temperature measurements, the sample was mounted in a continuous-flow helium cryostat equipped with a thermometer and heater near the cryostat tip, regulated by a temperature controller.

Experiments were performed in two polarizations: with light polarized parallel and perpendicular to the TCNQ chain axis. Infrared measurements were made at ten temperatures from 80 to 300 K, concentrating around T_c (220 K). In the near-infrared region (4000–15 000 cm^{-1}), data were collected at 100 and 300 K. Reflectance data for the visible frequency region were collected at room temperature. Thus, the total frequency range ran from 30 to 30 000 cm^{-1}.

Optical constants presented in this paper were obtained by, Kramers-Kronig analysis[14] of the power reflectance spectrum. This analysis allows the complex dielectric function,

$$\epsilon(\omega)=\epsilon_1(\omega)+i\epsilon_2(\omega)$$
$$=\epsilon_1(\omega)+\frac{4\pi i}{\omega}\sigma_1(\omega)\ ,$$

to be calculated. Here, ϵ_1 is the real part of the dielectric function and σ_1 is the frequency dependent conductivity. The low-frequency data were extrapolated to zero frequency assuming a constant reflectance, a common procedure for semiconducting materials. (Later in the text, we discuss a slight problem with this extrapolation method.) The high-frequency data were extended as $R\approx\omega^{-4}$ to simulate the extension toward infinity. Under the microscope, the samples were smooth, so no attempt was made to coat the surface with aluminum to correct for scattering loss.

III. RESULTS

A. Room-temperature spectra

Figure 1 displays the room-temperature reflectance over the entire spectral range for polarizations parallel and perpendicular to the stacking axis. For the electric-field vector polarized along the TCNQ chain direction, the spectra display two electronic excitations (at $\approx$3000 and $\sim$10 000 cm^{-1}). The low-energy band is very broad and contains a majority of the oscillator strength. These electronic features have been attributed to the transfer of charge within TCNQ tetramers in the stack.[15,16] At low frequency, the spectra display many sharp vibrational features. Ten of these modes are A_g vibrations of the TCNQ molecule, activated by coupling to the low-energy charge-transfer band.[9–11] Additional vibrational structure is much weaker and due to TCNQ modes of other symmetry[3] as well as those of the *N*-propylquinolinium donor cation.

Perpendicular to the TCNQ stacking direction, the reflectivity is low ($\approx$10%), flat, and almost featureless. The extreme anisotropy observed in NPrQn(TCNQ)$_2$ is observed for other TCNQ charge-transfer salts as well.[6]

B. Temperature dependence

The reflectance spectra exhibit gradual changes around T_c (220 K) as a function of temperature. In general, the spectral features become sharper and shift to higher frequency at lower temperature. The oscillator strength of the low-energy charge-transfer band increases systematically with decreasing temperature, especially in the low-temperature phase. The position of the deep minimum in the reflectivity (at $\sim$5500 cm^{-1}) is unaffected by tempera-

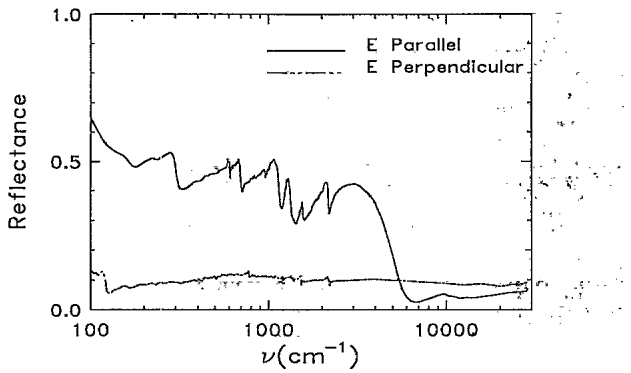

FIG. 1. Room-temperature reflectance of $NPrQn(TCNQ)_2$ with light polarized parallel and perpendicular to the TCNQ chain direction.

ture. Although the vibrational splitting appears only below T_c, it too becomes gradually more pronounced at lower temperature. No spectral hysteresis is observed upon temperature cycling.

To compare the spectral differences between the high- and low-temperature phases in the TCNQ stacking direction, the reflectivity and the frequency-dependent conductivity are shown in Fig. 2 for two temperatures, 300 and 100 K. The following discussion refers primarily to the frequency-dependent conductivity (in the lower panel of Fig. 2).

The character of the mid-infrared charge-transfer excitation is a strong function of temperature, indicating that important changes occur in the electronic state as a result of the phase transition. In the high-temperature phase, the low-energy charge-transfer band is very broad (due to the possible overlap of several excitations) and centered at $\sim 2200\ cm^{-1}$. At 100 K, the resonance sharpens and the center frequency shifts to a higher energy, the band center moving from 2200 cm^{-1} at 300 K and 2500 cm^{-1} at 100 K. Additionally, in the low-temperature phase, this band can be resolved into two components at 1000 and 2500 cm^{-1}, separated by a minimum at 1500 cm^{-1}. Similar behavior is observed in $MTPP(TCNQ)_2$.[17] At the same time, the integrated oscillator strength is significantly larger at 100 K than at 300 K.

A second charge-transfer band occurs at $\approx 9700\ cm^{-1}$ for both 300 and 100 K. In both phases, it appears as a weak doublet, the doublet structure being slightly more pronounced in the low-temperature phase. However, the general shape and oscillator strength of this band are not strongly affected by temperature.

The most obvious difference between the high- and low-temperature phases is the fundamental change in the infrared vibrational structure. Below T_c, each A_g phonon mode splits into a doublet. This fine structure becomes gradually more pronounced at lower temperature. No phonon splitting is observed in the high-temperature phase. Details of the typical doublet phonon structure in the low-temperature phase are presented in Fig. 3. At the lowest temperature, a well-developed sideband appears above each of the principal A_g peaks in $\sigma_1(\omega)$. For example, the main peak at approximately 1280 cm^{-1} is accompanied by a sideband at approximately 1400 cm^{-1}. With increasing temperature, both sidebands and main peaks lose oscillator strength. Above T_c, the sidebands are absent. Table I displays the unperturbed phonon frequencies and the amount of splitting of the sideband for several A_g phonon modes at 100 K. The unperturbed phonon frequencies were obtained from a plot of $\mathrm{Re}[1/\sigma(\omega)]$.[18]

The real part of the dielectric function, $\epsilon_1(\omega)$, is presented in Fig. 4. In the low-temperature phase, many of the infrared excitations result in a negative real dielectric function between the transverse (ω_{TO}) and optical (ω_{LO}), frequency of each mode. The mid-infrared charge-transfer excitation also drives $\epsilon_1(\omega)$ negative in both phases, although it is more pronounced in the low-temperature phase. This is evidence for a true plasma

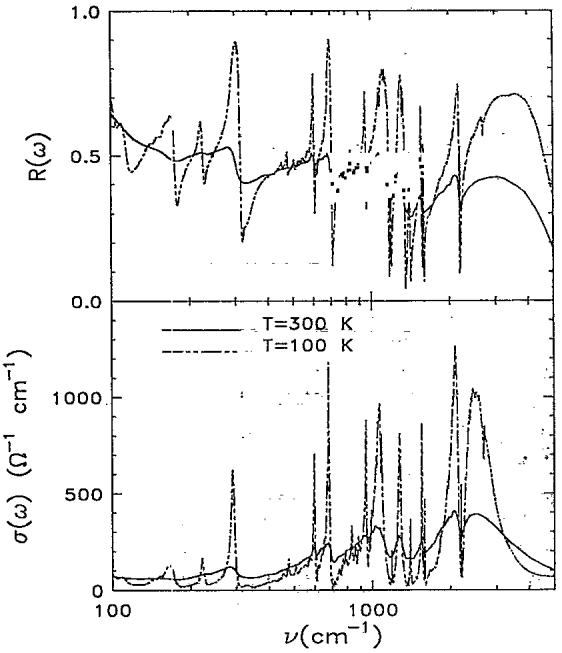

FIG. 2. Reflectance (upper panel) and frequency-dependent conductivity (lower panel) of $NPrQn(TCNQ)_2$ with light polarized along the chains at 100 and 300 K.

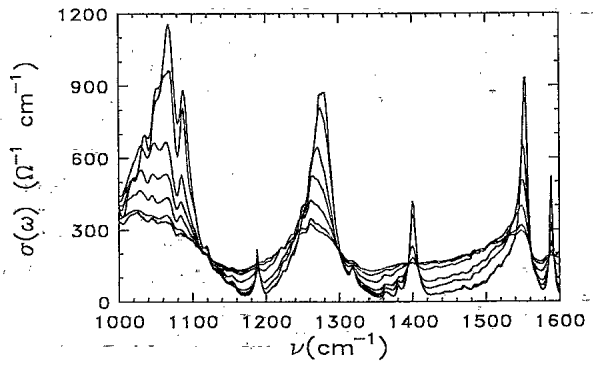

FIG. 3. Enlarged view of typical doublet structure in the frequency-dependent conductivity below the phase-transition temperature. Seven temperatures are shown: 210, 200, 190, 170, 150, 100, and 80 K.

TABLE I. A_g phonon mode splitting at 100 K.

A_g mode	ν_α (unperturbed)[a] (cm^{-1})	$\Delta\nu_{observ}$ (cm^{-1})	$\nu(TCNQ^0)$ (Ref. 9) (cm^{-1})	$\nu(TCNQ^-)$ (Ref. 10) (cm^{-1})
ν_2	2188.8	18.5	2229	2206
ν_3	1570.5	26.1	1602	1615
ν_4	1349.0	63.5	1454	1391
ν_5	1164.9	21.5	1207	1196
ν_6	958.6	17.2	948	978
ν_7	700.5	36.8	711	725
ν_8	606.0	31.5	602	613
ν_9	306.8			
ν_{10}	115.7			

[a]Obtained from plot of $\mathrm{Re}[1/\sigma(\omega)]$.

edge in the power reflectance at ≈ 4500 cm^{-1}. The screened plasma frequency is slightly blue shifted below T_c, as is typical in many semiconducting salts.[5] At high frequency, $\epsilon_\infty \approx 1.21$ and 1.17 in the high- and low-temperature phases, respectively. This indicates that there are no extremely intense electronic excitations above 30 000 cm^{-1}; otherwise, ϵ_∞ would be much greater than 1.0. Thus, the high-frequency $R \approx \omega^{-4}$ extrapolation is justified. Extrapolating the low-frequency far-infrared data to zero frequency, we estimate the static dielectric constant of the two phases to be between 30 and 10, depending on the details of the extrapolation. Above 300 cm^{-1}, $\epsilon_1(\omega)$ is unaffected by the choice of low-frequency extrapolation.

IV. DISCUSSION

A. Room-temperature spectra

Above T_c, the spectra of weakly metallic $NPrQn(TCNQ)_2$ show qualitative agreement with other quarter-filled, 1:2 semiconducting materials, such as $Qn(TCNQ)_2$,[12] $MEM(TCNQ)_2$,[11,19] $TeEA(TCNQ)_2$,[20] $TEA(TCNQ)_2$,[21,22] and $MTPP(TCNQ)_2$,[17] in terms of the position and intensity of the electronic and vibrational features. Although transport measurements show that $NPrQn(TCNQ)_2$ is weakly metallic in the high-temperature phase, the spectra are qualitatively different from typical spectra for conducting TCNQ salts. For example, low-frequency features commonly associated with highly conducting salts[3,4] include high reflectivity with a weakly superimposed vibrational structure (due to the screening of conduction electrons) and a Drude relaxation. Our spectra are not well described in these terms (see discussion below), evidence that the pronounced tetrameric clustering in $NPrQn(TCNQ)_2$ precludes a metallic band structure and introduces a semiconducting transport gap, 2Δ.

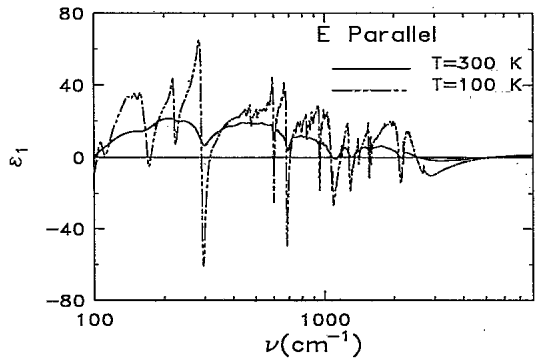

FIG. 4. Real part of the dielectric function, obtained by Kramers-Kronig analysis of the reflectance, for $NPrQn(TCNQ)_2$ with light polarized along the chains at 300 and 100 K.

1. Electronic features

In typical large-U semiconducting materials of this class, the high-energy spectral features in the TCNQ stacking direction consist of two strong, broad absorptions which correspond to electronic charge transfer between TCNQ moieties within the chain.[3,15,16] The absorption band centered at 2200 cm^{-1} corresponds to the charge transfer: $(TCNQ)^0+(TCNQ)^- \rightarrow (TCNQ)^- + (TCNQ)^0$. The breadth of the band may result from the overlap of two intratetramer charge-transfer excitations (at ≈ 1000 and 2200 cm^{-1}), as well as a low-energy intertetramer charge-transfer excitation (also at ≈ 2200 cm^{-1}). The low-energy charge-transfer excitation at 2200 cm^{-1} is of proper energy and significant intensity to couple with the TCNQ phonon modes.[11]

The band at $\approx 10\,000$ cm^{-1}, often seen as a weak doublet, is attributed[3,15,16] to the charge-transfer process: $(TCNQ)^- + (TCNQ)^- \rightarrow (TCNQ)^0 + (TCNQ)^{2-}$. The oscillator strength of this band is probably small because an electron has to hop two sites in order to occupy the same site as another electron. Because two electrons reside on the same site in the final state, the energy of this transition is proportional to $(U-V)$, the Hubbard parameters for on-site and nearest-neighbor Coulomb repulsion, respectively. Assuming V is small, we can estimate the on-site Coulomb repulsion from the center position of this band. We find $U=9700$ cm^{-1} (or 1.2 eV) for both phases of $NPrQn(TCNQ)_2$, which is comparable to the on-site Coulomb repulsion energy in other TCNQ charge-transfer salts.[6,4] The higher-energy charge-transfer excitation is not strongly temperature dependent.

2. Electron-phonon coupling

Upon comparison of the infrared electron-molecular vibration-coupling-induced modes with other semiconducting quarter filled 1:2 salts, it becomes clear that the intratetramer charge-transfer bands interact with the A_g molecular vibrations.[11–24] All ten A_g modes are observed in $NPrQn(TCNQ)_2$, most with relatively strong intensity. The intensities and frequencies of the excitations are in relatively close agreement to the previously studied 1:2 semiconducting compounds listed above,[11,12,17,19–22] implying that the electron-phonon coupling constants are of similar size in these different salts.[25]

The infrared spectra of semiconducting TCNQ salts are dominated by electron localization effects,[3–6] suggesting that the TCNQ stack can be modeled as linear clus-

ters of dimers or tetramers. The solution of the electron-phonon interaction for an isolated TCNQ dimer with one electron per two TCNQ molecules has been presented by Rice *et al.*,[11] the final result of which is an expression for the frequency-dependent conductivity. Successful application of the Rice dimer model to the experimental frequency-dependent conductivity in the chain axis direction indicates that dimerized quarter-filled salts may be understood as an electron-phonon interaction of one electron on an isolated dimer.

However, application of the isolated dimer model to our frequency-dependent conductivity data for $NPrQn(TCNQ)_2$ is unsatisfactory, with especially poor agreement below 1000 cm^{-1} (Fig. 5). This suggests that $NPrQn(TCNQ)_2$ should not be considered as an isolated dimer in a $4k_f$ configuration with one electron on two sites, and that the interdimer interactions are too strong to neglect. This result was not unexpected; although $NPrQn(TCNQ)_2$ has a quarter-filled band, the TCNQ chain is composed of relatively isolated *tetramers.*

The concept of electron-molecular vibrational coupling has been extended by Yartsev[23,24] to describe isolated tetramers. The calculation, obtained using this model, is shown in Fig. 5. The model parameters are listed elsewhere.[26] The good agreement with our experimental spectrum suggests that $NPrQn(TCNQ)_2$ is a system of relatively isolated TCNQ tetramers, occupied by two electrons, and that intratetramer interactions dominate the optical properties of the salt.

3. *Low-frequency behavior*

Extrapolating the ac conductivity to zero frequency, we obtain an estimate of the dc conductivity of ≈ 50 $\Omega^{-1}\,cm^{-1}$ at 300 K. This value is significantly greater ($\times 200$) than that obtained by four probe measurements.[1,2]

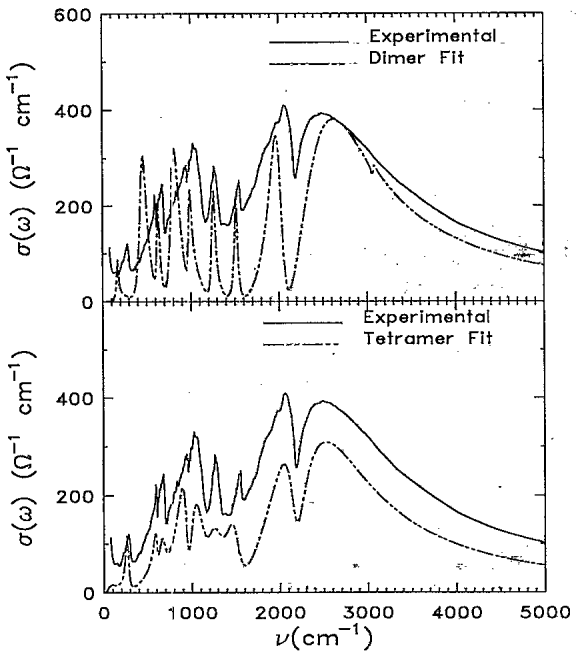

FIG. 5. Upper panel: Isolated dimer model fit to the frequency-dependent conductivity at 300 K. Lower panel: Isolated tetramer model fit to the frequency-dependent conductivity at 300 K.

If the data are truncated at 250 cm^{-1} and the Kramers-Kronig analysis redone using identical low- and high-frequency extrapolations, we obtain $\sigma_1(0) \approx 0.1$ $\Omega^{-1}\,cm^{-1}$, a value which is in good agreement with the four-probe dc conductivity. The spectral results are unmodified at higher frequency (above 300 cm^{-1}).

We believe that this inconsistency is a direct result of the unusual low-frequency reflectance. As seen in Fig. 2, the reflectance rises sharply below ≈ 250 cm^{-1}, saturating at about 70% reflectance. The temperature dependence of this low-frequency relaxation undergoes a gradual transition between the high- and low-temperature phases, analogous to the temperature dependence of the dc conductivity; the strongest relaxation is at 230 K, directly above T_c. This unusual upturn in the low-frequency reflectance may be attributable to disorder near the Fermi surface.[27] Unfortunately, the small crystal size prevented measurements below 60 cm^{-1}. The optical constants presented in this paper are the result of Kramers-Kronig transform on the data over the entire frequency range of 60–30 000 cm^{-1}.

B. Low-temperature phase

1. *Electronic structure*

The temperature dependence of the charge-transfer bands indicates important changes in the electronic structure of the salt as a result of the phase transition. Below T_c, the low-energy charge-transfer band can be resolved into two main bands, centered at 1000 and 2500 cm^{-1}, respectively. They are separated by a minimum in the frequency-dependent conductivity at 1500 cm^{-1}. Świetlik and Graja have observed a similar two-banded structure in both phases of tetrameric $MTPP(TCNQ)_2$.[17]

As in the high-temperature phase, we expect two intratetramer and one intertetramer charge-transfer bands. Although the intratetramer distances are identical at 100 K, the mode of overlap is different.[8] Consequently, two distinct intratetramer charge-transfer excitations are still expected. We have assigned the band at ≈ 1000 cm^{-1} to intratetramer charge transfer; the band at 2500 is probably composed of overlapping intratetramer and intertetramer excitations.

Below T_c, the increased oscillator strength of these bands is indicative of a larger intratetramer transfer integral, consistent with structural studies in the low-temperature phase[7] which conclude that intratetramer distances decrease as the chains become more uniformly tetramerized. From the systematic increase in the oscillator strength of the low-energy charge-transfer band below T_c, we can infer a gradual change in the intratetramer distances. The band sharpening below T_c is a characteristic commonly associated with charge localization.

2. *Vibrational features*

The A_g vibrational lines split into doublets below T_c. As seen in Fig. 3, the oscillator strength is unevenly di-

vided between the two peaks of the doublet; in every case, the lower-energy resonance is much more intense. Within the doublet, the higher-energy sideband gradually grows in intensity as temperature decreases, but its resonance frequency remains constant. The resonance frequency of the more intense main mode gradually increases as temperature decreases; thus, the energy difference between the main peak and the sideband decreases with decreasing temperature below T_c. This splitting behavior is qualitatively seen in all of the doublet modes.

Such phonon splitting behavior has been previously observed[17,22,28] in the low-temperature phases of other organic charge-transfer salts, and is generally attributed to an unevenly localized charge distribution within the tetramer repeat unit.[23,24,28]. The unperturbed A_g phonon frequencies and splitting energies, shown in Table I, support this claim. Comparison of these values with the frequency difference expected from isolated $(TCNQ)^0$ and $(TCNQ)^-$ molecules[9,10] shows that the doublet frequency separation is of reasonable size. Consequently, the fine structure in $NPrQn(TCNQ)_2$ presents evidence for two distinct molecular environments of different charge within the tetramer.

The possibility that the splitting of the vibrational lines is a consequence of the coupling of the A_g vibrational modes with *two* low-energy charge-transfer excitations should not be ignored. Examination of Fig. 2 will show that, although there is a weak band centered at 1000 cm^{-1} in the low-temperature phase, it is well separated in frequency from the main charge-transfer band at 2500 cm^{-1}, and thus, is unlikely to couple to the phonon motion. If it were involved in the coupling, we would expect to see A_g multiplets, not doublets. Alternately, the A_g phonon splitting may be due to steric interactions of the donor cations with the TCNQ stack. However, this is also unlikely, as structural studies[7,8] reported no significant changes in the behavior of the NPrQn cation as a function of temperature.

Thus, we believe that the doublet splitting pattern below T_c is directly related to the modification of the original charge distribution by localization within the tetramer, probably on every other site. (The absence of A_g mode splitting in the infrared spectra of the high-temperature phase could also be taken as evidence for site indistinguishability.)

3. *Sum rule*

Information about the effective number of electrons involved in optical transitions can be obtained from the partial sum rule[14]

$$\left[\frac{m}{m^*}\right] N_{\text{eff}}(\omega)=\frac{m}{32\pi N_c e^2}\int_0^{\omega}\sigma_1(\omega')d\omega' ,$$

where m^* is the effective mass of the carriers and N_c is the carrier density. From structural data,[7,8] we obtain, for $NPrQn(TCNQ)_2$, $N_c=1.33\times10^{21}$ cm^{-3} in the high-temperature phase and $N_c=1.39\times10^{21}$ cm^{-3} in the low-temperature phase. A plot of the oscillator strength sum rule is shown in Fig. 6 for the electric-field vector parallel to the chain direction at 300 and 100 K, as well as perpendicular at 300 K.

In the chain direction, $(m/m_*)N_{\text{eff}}$ rises rapidly in the low-frequency region, leveling off in the near infrared. Despite the appearance of the doublet pattern and the sharpening of the phonon modes in the low-temperature phase, the integrated oscillator strength below the charge-transfer band is not a strong function of temperature. In the high-temperature phase, the broad absorption due to overlapping charge-transfer excitations is evident. Below T_c, two distinct charge-transfer absorptions can be resolved, and the increased oscillator strength of the charge-transfer band centered at 2500 cm^{-1} is also clear. From the plateau values of the integrated oscillator strength in the near infrared and $N_{\text{eff}}=0.5$, we estimate $m^*=1.35m_e$ and $m^*=1.1m_e$ in the high- and low-temperature phases, respectively. The change in oscillator strength associated with the U band is small. At higher frequencies, the two curves come together nicely, demonstrating conservation of oscillator strength above and below T_c. In the polarization perpendicular to the chain axis, $(m/m^*)N_{\text{eff}}$ is small in the infrared but rises rapidly at higher frequencies.

C. Implications for charge transport

The spectra of $NPrQn(TCNQ)_2$ are clearly characteristic of a semiconductor in the high-temperature phase, but it is not a straightforward matter to assign an optical gap, as it appears to be broadened and obscured. We believe that the broadening is the result of the overlap of three distinct charge-transfer bands, representing the two different intratetramer and one intertetramer charge-transfer excitation, respectively.

Because conduction is limited by intertetramer hopping, an optical estimate for the semiconducting energy gap can be obtained by linear extrapolation from the shoulder of the band associated with intertetramer transport in Fig. 2. (It can also be obtained from examination of the sum rule in Fig. 6.) Using this method, we obtained $2\Delta\approx800\pm200$ cm^{-1} at 300 K. Alternately, the gap position can be estimated from the changes in the

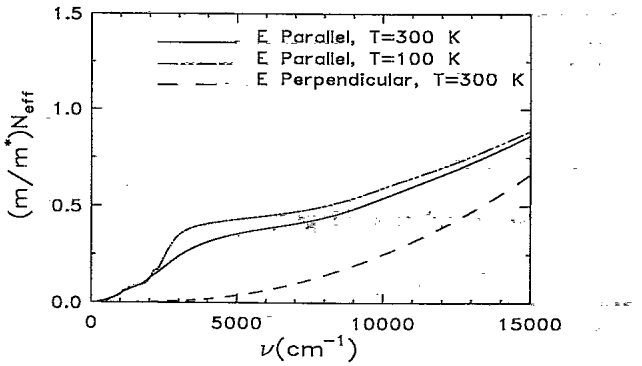

FIG. 6. Sum rule for the chain axis polarization at 300 and 100 K and for the short axis polarization at 300 K.

phonon line shape: below the gap, phonons have a typical Lorentizian shape; above the gap, overlap with the electronic feature perturbs the excitation, resulting in a Fano[29] line shape. Using this method, we obtain a comparable estimate of the semiconducting gap.

In the low-temperature phase, we can distinguish the various band shapes more clearly. Extrapolation of the leading edge of the charge-transfer band associated with intertetramer hopping (in Figs. 2 or 6) provides us with an estimate of the semiconducting energy gap at 100 K; we find $2\Delta \approx 1800$ cm^{-1} at 100 K, consistent with transport measurements.[1,2]

D. Comparison with previous results

In this section, we discuss our spectral studies of NPrQn(TCNQ)$_2$ with respect to the previous results on the closely related quarter-filled compounds Qn(TCNQ)$_2$ and (NMP)$_x$(Phen)$_{1-x}$(TCNQ).[12,30–34] Although the previous measurements by McCall *et al.* were performed on KCl pellets due to small crystal size, many useful comparisons can be made.

Despite the chemical modifications of the donor cation and the significantly different dc conductivities, the 300-K spectra of NPrQn(TCNQ)$_2$, Qn(TCNQ)$_2$, and (NMP)$_x$(Phen)$_{1-x}$(TCNQ) are similar in character and typical of semiconducting charge-transfer salts. In the infrared, all three of the aforementioned materials have infrared-active A_g vibrational features, although they are less pronounced in Qn(TCNQ)$_2$ and (NMP)$_x$(Phen)$_{1-x}$(TCNQ) due to screening by conduction electrons. Excitations at higher energy can be assigned to charge transfer in the TCNQ chain in these large-U materials. McCall *et al.* estimate $2\Delta \approx 700$–950 cm^{-1} for Qn(TCNQ)$_2$, in excellent agreement with our estimate for the NPrQn salt at 300 K. The authors attribute the gap in both Qn(TCNQ)$_2$ and (NMP)$_x$(Phen)$_{1-x}$(TCNQ) to a combination of a Peierls distortion and the external cation potential. It is expected that the semiconducting gap in NPrQn(TCNQ)$_2$ is of similar origin.

There are many similarities in the low-temperature spectra of these materials as well. As in NPrQn(TCNQ)$_2$, the A_g vibrational features of Qn(TCNQ)$_2$ and (NMP)$_x$(Phen)$_{1-x}$(TCNQ) become more pronounced at lower temperature. From plots of the normalized A_g model oscillator strength versus temperature, the authors conclude that the strength of the Peierls interaction, and thus the size of the transport gap, increases with decreasing temperature. Qualitatively similar behavior is found in NPrQn(TCNQ)$_2$ as well. For Qn(TCNQ)$_2$ and (NMP)$_x$(Phen)$_{1-x}$(TCNQ), the gradual decay of the gap with temperature has been ascribed to the presence of thermal and chemical solitons.[32,33] The role of soliton defect states in NPrQn(TCNQ)$_2$ is still under investigation.

Although these materials are chemically very closely related, the temperature dependence of the electron-phonon coupling is strikingly different indicating important changes in the fundamental interactions in these materials. As previously mentioned, the vibrational features in these salts become more intense with decreasing temperature. However, NPrQn(TCNQ)$_2$ has less (rather than more) residual conductivity below the gap than the other two quinoid-based charge-transfer salts at lower temperature. This is probably related to the lower dc conductivity. The A_g vibrational modes in NPrQn(TCNQ)$_2$ also provide evidence for a structural phase transition. At T_c (220 K), the A_g phonon modes of NPrQn(TCNQ)$_2$ split into doublets, evidence for a change in the charge distribution within the tetramer. No such dramatic changes are observed in the electron-phonon coupling in Qn(TCNQ)$_2$ or (NMP)$_x$(Phen)$_{1-x}$(TCNQ) as a function of temperature.

The very low-frequency absorption of Qn(TCNQ)$_2$ and (NMP)$_x$(Phen)$_{1-x}$(TCNQ) is small, and based upon this observation, the authors conclude that a gap exists in the density of states at the Fermi level. This is contrasted by an unusual increase in the low-energy frequency-dependent conductivity in NPrQn(TCNQ)$_2$, which may indicate the importance of disorder near the Fermi surface.[27] Such disorder would strongly affect the infrared and physical properties of this material.

The temperature-dependent dc conductivity of Qn(TCNQ)$_2$ and (NMP)$_x$(Phen)$_{1-x}$(TCNQ) has been fit to a two-component model by Epstein and Conwell in which σ_T is a product of a strongly temperature-dependent mobility and an activated carrier concentration.[35,36] The expression is given as

$$\sigma_T = ne\mu = \sigma_0 T^{-\alpha} \exp\left[\frac{-\Delta}{k_B T}\right] .$$

Although such a model for the temperature dependence of the dc conductivity would seem to provide a plausible framework for the observed metal-like transport properties and semiconductorlike spectra, which characterized NPrQn(TCNQ)$_2$, a fit of this model to the experimental data[1] is, overall, unsatisfactory. In the high-temperature phase, we obtain a relatively good quality fit, with parameters $\Delta \approx 1190$ K and $\alpha = 4.0$. However, near and below T_c, the model conductivity does not fall enough to give a reasonable fit to the data. Perhaps a better fit to the NPrQn(TCNQ)$_2$ data would be obtained using a temperature-dependent activation energy, Δ.

E. The phase transition

The behavior of the A_g phonon modes is a strong function of temperature in NPrQn(TCNQ)$_2$. Experimentally, the doublet structure of the A_g phonon modes appears in the spectra only below 200 K and is clearly a characteristic feature of the electronic structure below T_c.

Changes in these A_g modes are directly related to fundamental characteristics of the phase transition. In similar studies of TCNQ salts, Bozio and Pecile have shown that the intensity of the satellite band is proportional to the square of the order parameter.[37,38] In our case, it seems reasonable to define the charge difference between the two inequivalently charged TCNQ ions in the tetramer as the order parameter of the structural phase transition. This is analogous to defining the order parameter as

the change in the static charge-density-wave amplitude, observed in charge-density-wave materials such as TTF-TCNQ.[39]

A more detailed examination of the typical phonon doublet structure of $NPrQn(TCNQ)_2$ below T_c is given in this section. As shown in Fig. 3, each A_g peak splits into a main phonon mode and a less intense, higher-energy satellite mode in the low-temperature phase. The integrated spectral intensity of the satellite mode grows systematically with decreasing temperature below T_c. The oscillator strengths of four modes versus the temperature are shown in Fig. 7. In this plot, the oscillator strengths have been normalized with respect to the limiting low-temperature value of the intensity of each mode. The error in the oscillator strength at each temperature is estimated to be ±4%.

We can conclude from the gradual variation of the integrated spectral intensity of the satellite mode with temperature that the order parameter of the phase transition also changes gradually with temperature. Thus, the structural phase transition is of second order, in agreement with previous work.[1,2] Additional evidence for this conclusion is found in the very systematic change of the entire infrared reflectance spectrum through the phase transition; with no hysteresis observed on temperature cycling.

V. CONCLUSION

We have presented a spectral investigation of $NPrQn(TCNQ)_2$ at various temperatures both above and below T_c in an effort to understand the unusual electrical transport properties in the high- and low-temperature phases and gain insight into the characteristics of the phase transition. In the high-temperature phase, our spectra are typical of other quarter-filled 1:2 semiconducting TCNQ charge-transfer salts, with a uniform charge distribution on the tetramer above T_c. The broad low-energy charge-transfer band is attributed to three overlapping excitations.

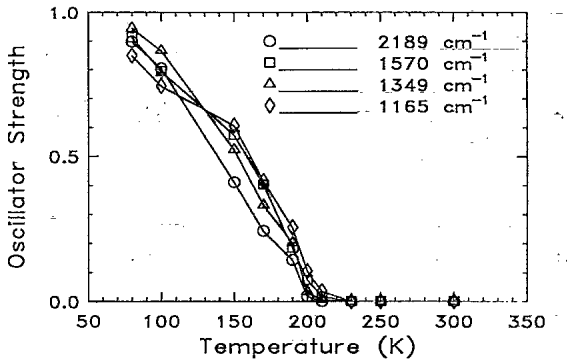

FIG. 7. Normalized intensity of sideband modes associated with four characteristic A_g phonon excitations vs temperature.

In the low-temperature phase, the low-energy charge-transfer band is resolved into two separate bands, separated by a minimum in the frequency-dependent conductivity. The bands have been attributed to intratetramer and intertetramer charge transfer. The increased oscillator strength of the low-energy charge-transfer band is evidence of an increased intratetramer transfer integral. The doublet fine structure of the phonon modes is indicative of an uneven (and more localized) charge distribution within the tetramer.

Spectrally, $NPrQn(TCNQ)_2$ is a semiconductor in the high-temperature phase. We attribute the weakly metallic transport properties above T_c to the uniform charge distribution within the tetramer and the high degree of overlap between the intratetramer and intertetramer charge-transfer bands. $NPrQn(TCNQ)_2$ is a semiconductor in the low-temperature regime as well, but transport is hindered by charge localization which may reduce the overlap of the low-energy charge-transfer bands.

[1]M. Eró-Gecs, L. Forró, Gy. Vancso, K. Holczer, G. Milály, and A. Jánossy, Solid State Commun. **32**, 845 (1979).
[2]A. Jánossy, G. Mihály, L. Forró, J. R. Cooper, M. Miljak, and B. Korin-Hamzic, Mol. Cryst. Liq. Cryst. **85**, 1623 (1982).
[3]V. M. Yartsev and R. Świetlik, Rev. Solid State Sci. **4**, 69 (1990).
[4]C. S. Jacobsen, in *Semiconductors and Semimetals*, edited by E. M. Conwell (Academic, New York, 1985) Vol. 27, Chap. 5.
[5]R. Bozio and C. Pecile, in *Spectroscopy of Advanced Materials*, edited by R. J. H. Clark and R. E. Hester (Wiley, Chichester, 1990).
[6]D. B. Tanner, in *Extended Linear Chain Compounds*, edited by J. W. Miller (Plenum, New York, 1982), Chap. 5.
[7]T. Sundaresan and S. C. Wallwork, Acta Crystallogr. B **28**, 1163 (1972).
[8]G. Rindorf, N. Thorup, and K. Kamarás, Synth. Met. **25**, 189 (1988).
[9]A. Girlando and C. Pecile, Spectrochim. Acta A **29**, 1859 (1975).
[10]R. Bazio, I. Zanon, A. Girlando, and C. Pecile, J. Chem. Soc. Faraday Trans. II **74**, 235 (1978).
[11]M. J. Rice, V. M. Yartsev, and C. S. Jacobsen, Phys. Rev. B **21**, 3437 (1980).
[12]R. P. McCall, I. Hamberg, D. B. Tanner, J. S. Miller, and A. J. Epstein, Phys. Rev. B **39**, 7760 (1989).
[13]K. D. Cummings, D. B. Tanner, and J. S. Miller, Phys. Rev. B **24**, 4142 (1981).
[14]F. Wooten, *Optical Properties of Solids* (Academic, New York, 1972).
[15]Y. Iida, Bull. Chem. Soc. Jpn. **42**, 637 (1969).
[16]J. Tanaka, M. Tanaka, T. Kawai, T. Takabe, and O. Maki, Bull. Chem. Soc. Jpn. **49**, 2358 (1976).
[17]R. Świetlik and A. Graja, J. Phys. (Paris) **44**, 617 (1983).
[18]V. M. Yartsev and C. S. Jacobsen, Phys. Status Solidi B **145**, K149 (1988).
[19]V. M. Yartsev and C. S. Jacobsen, Phys. Rev. B **24**, 6167 (1981).
[20]V. Železný, J. Petzelt, and R. Świetlik, Phys. Status Solidi B **140**, 595 (1988).
[21]A. Brau, P. Bréusch, J. P. Farges, W. Hinz, and D. Kuse,

Phys. Status Solidi B **62**, 615 (1974).
[22]M. V. Belousov, A. M. Vainrub, and R. M. Vlasova, Fiz. Tverd. Tela (Leningrad) **18**, 2637 (1976).
[23]V. M. Yartsev, Phys. Status Solidi B **126**, 501 (1984).
[24]V. M. Yartsev, Phys. Status Solidi B **149**, 157 (1988).
[25]A. Painelli, A. Girlando, and C. Pecile, Solid State Commun. **52**, 801 (1984).
[26]K. Kamarás, C. S. Jacobsen, V. Železný, J. L. Musfeldt, and D. B. Tanner, Synth. Met. **42**, 1839 (1991).
[27]A. N. Bloch, R. B. Weisman, and C. M. Varma, Phys. Rev. Lett. **28**, 753 (1972).
[28]V. M. Vartsev and M. J. Rice, Phys. Status Solidi B **100**, K97 (1980).
[29]V. Fano, Phys. Rev. **124**, 1866 (1961).
[30]R. P. McCall, D. B. Tanner, J. S. Miller, A. J. Epstein, I. Howard, and E. M. Conwell, Mol. Cryst. Liq. Cryst. **120**, 59 (1985).
[31]R. P. McCall, D. B. Tanner, J. S. Miller, A. J. Epstein, I. A. Howard, and E. M. Conwell, Synth. Met. **11**, 231 (1985).
[32]E. M. Conwell and I. A. Howard, Phys. Rev. B **31**, 7835 (1985).
[33]E. M. Conwell and I. A. Howard, Synth. Met. **13**, 71 (1986).
[34]A. J. Epstein, R. W. Bigelow, J. S. Miller, R. P. McCall, and D. B. Tanner, Mol. Cryst. Liq. Cryst. **120**, 43 (1985).
[35]A. J. Epstein, E. M. Conwell, D. J. Sandman, and J. S. Miller, Solid State Commun. **23**, 355 (1977).
[36]A. J. Epstein, E. M. Conwell, D. J. Sandman, and J. S. Miller, Solid State Commun. **24**, 627 (1977).
[37]R. Bozio and C. Pecile, Solid State Commun. **37**, 193 (1981).
[38]R. Bozio and C. Pecile, J. Phys. C **13**, 6205 (1980).
[39]M. J. Rice, Phys. Rev. Lett. **37**, 36 (1976).